SDR-BASED PRN P-BAND RADAR FOR EARTH OBSERVATION

Edwar Edwar[1,2], Yasir M. O. Abbas[2], Shah Zahid Khan[2], Ashwaq Alkaabi[2,6], Abdul-Halim Jallad[2], Adriano Camps[3,4,5]

[1]School of Electrical Engineering, Telkom University, Bandung, Indonesia
[2] Department of Electrical and Communication, United Arab Emirates University, Al Ain, UAE
[3]CommsSens Lab, UPC, Dept. of Signal Theory and Communications, BarcelonaTech, Barcelona.
[4]Institut d'Estudis Espacials de Catalunya IEEC/CTE-UPC, Barcelona.
[5]ASPIRE Visiting International Professor, United Arab Emirates University, CoE, Al Ain, UAE.
[6]Engineer Researcher, Science and Technology Center, Ministry of Defense, Abu Dhabi, UAE

ABSTRACT

P-band radars around 435 MHz are receiving an increased interest for Earth observation because they can penetrate the forest canopy and penetrate the soil down to the root zone, allowing to monitor subsurface soil moisture, which is of crucial for crop irrigation management. However, P-band radars face some challenges, such as the potential radio interference (RFI) from long-range radars or radio-amateur emissions, and, because of the long wavelength ~70 cm, they also require large antennas. In this paper, a novel approach using a long sequence Pseudo-Random Noise (PRN) waveform is proposed to mitigate the RFI issue and improve co-existence between different radars, while allowing to reduce the transmitted peak power. This paper presents the P-band SDR polarimetric interferometric ground-based synthetic aperture radar (Pol-In GB-SAR) that has been designed, and it is being developed by the UAE University. Furthermore, the proposed radar system was configured by using GNU Radio, an open-source software. This method has reduced the radar system development process and cost.

Index Terms— SDR, GNU Radio, PRN, P-Band, GBSAR.

1. INTRODUCTION

Up to present, space-borne SARs are mostly working at L, S, C, and X-band (Table 1). The opportunity to explore lower frequency band such as P-band is widely open recently. This band has a longer wavelength which makes it sensitive to forest trunks and soil moisture better than other higher frequencies are. This band is also able to penetrate the ground, enabling sub-surface object detection applications.
However, the risk of RFI is higher than at other existing SAR bands because of the member of adjacent services.
The RFI impact on SAR imagery is an unusual footprint on the image where the RFI occurs. One of the examples is the mutual interference between Sentinel-1 and Radarsar-2 satellite [1]. Other RFI problems on at the other bands have also been reported [2], [3], [4]. RFI might also exist at P-band as there are many services such as amateur radio communications and ISM devices. Therefore, our SAR has to be designed keeping in mind the RFI issues from the very beginning.

Table 1. Existing SAR Satellite.

Satellite	Frequency	Launch Year
TerraSAR X[5]	X-Band / 9.65 GHz	2007
Tandem X[5]	X-Band / 9.65 GHz	2010
Radarsat-2[6]	C-Band / 5.405 GHz	2007
COSMO-skymed[7]	X-Band / 9.6 GHz	2007
RISAT-1[8]	C-Band / 5.35 GHz	2012
ALOS-2 PALSAR-2[9]	L-Band / 1.2 GHz	2014
Sentinel-1A[10]	C-Band / 5.405 GHz	2014
Sentinel-1B[10]	C-Band / 5.405 GHz	2016
GAOFEN-3[11]	C-Band / 5.4 GHz	2016
SAOCOM[12]	L-Band / 1.275 GHz	2018
PAZ SAR[13]	X-Band / 9.65 GHz	2018
ICEEYE[14]	X-Band / 9.65 GHz	2018
NovaSAR-1[15]	S-Band / 3.1 GHz	2018
RCM[16]	C-Band / 5.405 GHz	2019

Radar development is normally done for a specific configuration and frequency, and it is costly to change its configuration because components have to be replaced. However, since the Software Defined Radio (SDR) was introduced, the flexibility in radar system development has improved. SDRs are reconfigurable radio devices whose configuration can be modified by a program. SDR contains a radio module and an FPGA or a System-on-Chip (SoC) [17]. Nowadays, SDR module is widely available in the market with affordable prices. In radar research and development, the use of SDR is becoming popular as exemplified by [18], [19], [20], [21], and [22].

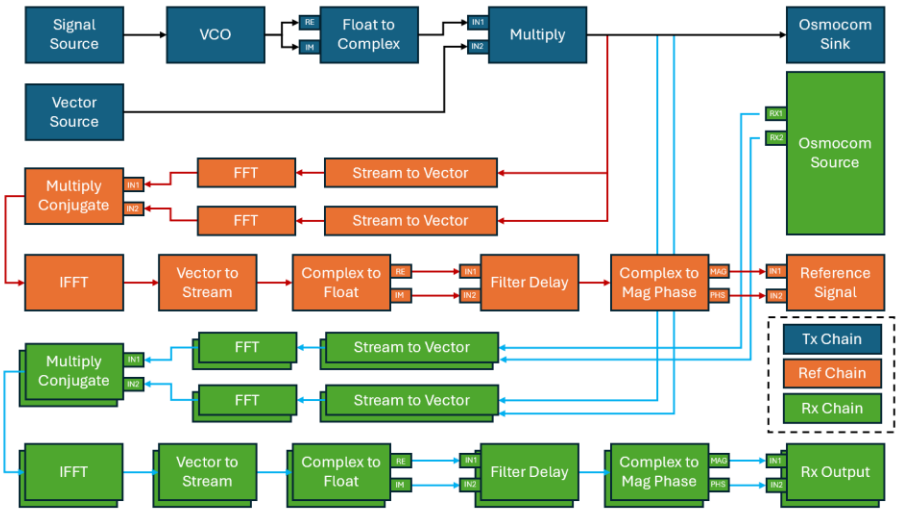

Figure 1. PRN Radar Design with Synchronization Block.

In this paper, a ground-based polarimetric and interferometric (Pol-In) SAR system is presented. This Pol-In SAR was developed on a SDR platform. The transmitted signal is a PRN and it was selected due to its characteristics that make it robust to the RFI. PRN signals are commonly used in global navigation satellite systems (GNSS) and CDMA communications. In order to perform interferometry to obtain the height of detected objects, two receivers and two receiving antennas are used. As said, an SDR platform is used to reduce the radar development complexity.

2. RADAR SYSTEM DESIGN

The radar block system was designed using the GNU Radio software [23]. This is an open-source application able to access some SDR modules for various purposes. Table 2 presents the parameters of the proposed PRN radar design. Figure 1 shows the design of the radar system. It consists of a pulse shaping system on the transmitter. In every receiver device, there is a matched filter, and synchronization block. on the receiver. The matched filter is implemented using a correlator block on both channels, using two FFTs for the transmitted and received signals, which are multiplied, and then its inverse FFT computed. The synchronization process is done afterwards using "*Filter Delay*" block which equalizes the delay in both branches.

3. IMPLEMENTATION AND EXPERIMENTAL RESULTS

The radar block system that was explained in the previous section has been implemented by using a BladeRF [24]. BladeRF is an SDR module that works from 30 MHz to 6 GHz of frequency. It has two transmitter ports and two receiver ports. Figure 3 shows the SDR setup done in this research. Two BladeRFs are used to accommodate two receiver chains. It will be useful for enabling the interferometry function.

Table 2. PRN Radar Parameters.

Parameter	Unit		Value
Frequency Center (f_0)	MHz	f_0	435
Pulse Repetition Frequency	Hz	PRF	500
PRN Length	sample		32768
Bandwidth	MHz	$2/T_c$	32.768
Chip Period	ns	1/PRF/PRN Length	61.0352
Frequency Sampling	MHz	$1/T_c$	16.384

In Figure 2, the supporting RF modules are used to manage the flow of the transmitted and received signal. It consists of bandpass filter (BPF), coupler, splitter, limiter, and amplifier. At the end, the radar system is connected with one transmitter antenna and two receiver antennas. The antenna used is dual polarization cross-yagi antenna (Fig. 3).

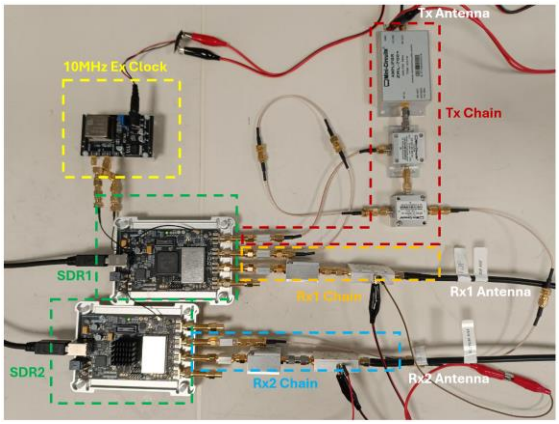

Figure 2. SDR and RF Front End Setup

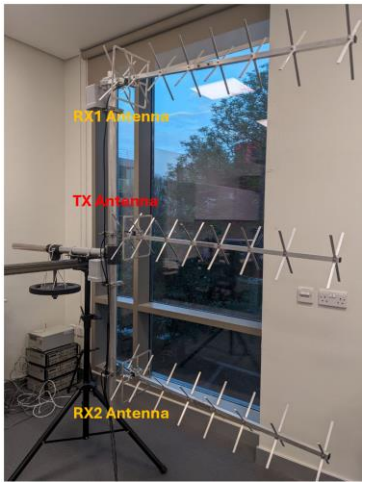

Figure 3. Antenna Configuration

Figures 4 and 5 show the transmitter and receiver synchronization result. In Figure 4, the phase of the echo is unstable. It was stabilized by integrating a "Filter Delay" block, as shown by Figure 5. Now, the phase is within $+\pi/2$ or $-\pi/2$ (0° to 180° equivalently), corresponding to the PRN signal, and the peaks are more clearly observed.

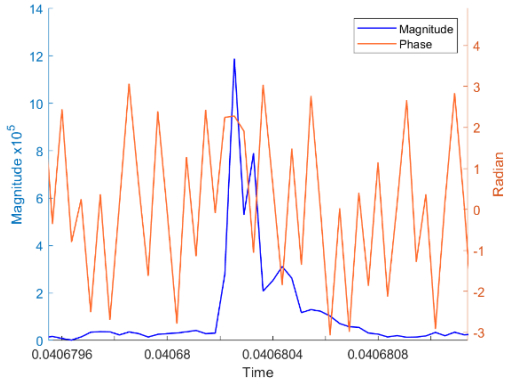

Figure 4. PRN Radar Magnitude and Phase before Synchronization

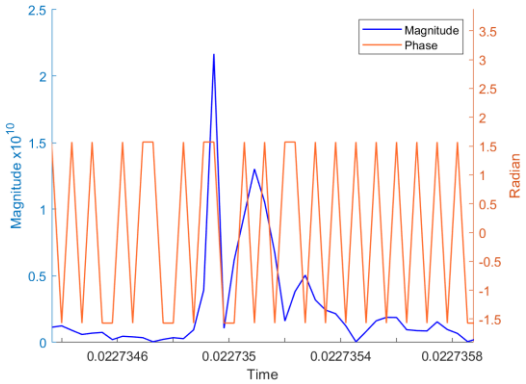

Figure 5. PRN Radar Magnitude and Phase after Synchronization

The next processing step after the transmitter and the receivers have been synchronized is the calibration of the echoes. It was done by selecting the first echo as the reference pulse, then the following complex echoes are normalized with respect to it (Fig. 6). The following process has been done was integrating incoming echoes to increase the SNR. In this experiment, 47 echoes have been coherently integrated by adding this matrix by columns, as shown by Figure 7.

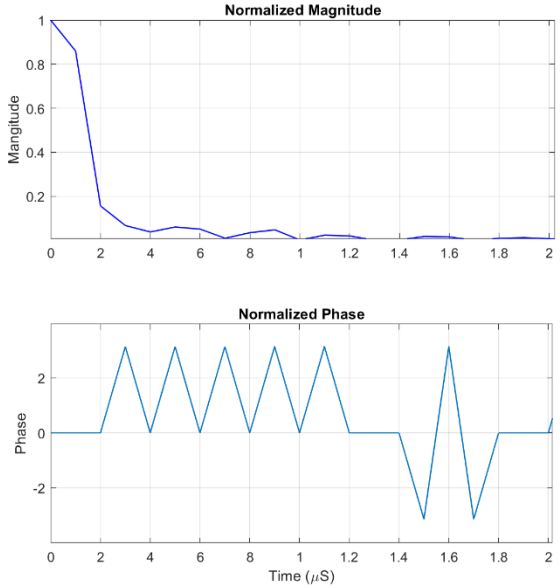

Figure 6. PRN Radar Normalization Result: Magnitude (Top Figure), and Phase (Bottom Figure).

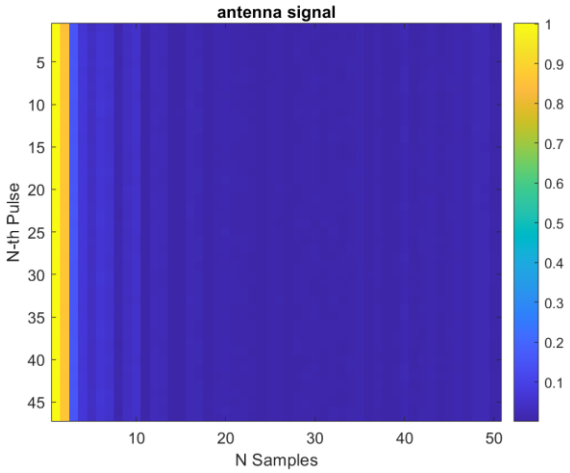

Figure 7. PRN Radar Echoes Piled Up for Coherent Integration (by Columns).

A design of radar antenna has been investigated. This antenna will be a crucial part in the future as the PRN radar is projected to be launch. The antenna type is microstrip array antenna. It forms 2 × 4 antenna array layout, as shown by Figure 8. Each element is made of a rectangular patch. The PCB material was a dielectric of 3.5 of the flexible substrate polyimides, and its total thickness of 2 mm. The antenna was

designed to work at 1.275MHz. The simulated return loss result on Figure 8 is between -10dB to -30dB. The design can further be optimized, by either adjusting the microstrip line or increasing the spacing between the patches.

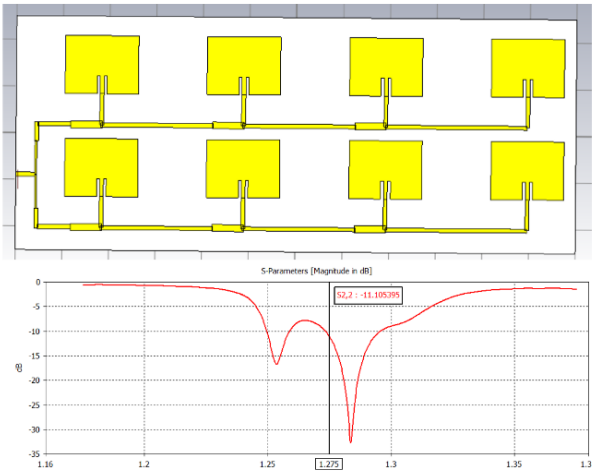

Figure 8. The 2 × 4 Microstrip Array Antenna (Top Figure) and its Simulated Return Loss Result (Bottom Figure).

4. FUTURE WORKS

This P-band Pol-In GB-SAR development is on progress, and it is expected to be completed by 2025. Thereafter, it will be used for ground validation of the ESA Biomass mission in desertic areas. This system is also part of a long-term plan that includes the development of drone-based SAR by 2027, and airborne-based one by 2029, and a CubeSat-based one by 2032 (Fig. 8) which will be deployed in a parallel activity.

Figure 8. PRN Radar Research Roadmap

5. CONCLUSIONS

The time synchronization, and amplitude/phase calibration in an PRN SDR-based radar using GNU Radio software has been presented. The synchronization process was implemented by utilizing the "*Filter Delay*" block, while the amplitude and phase calibration have been performed by normalizing the cross-correlation of the received signals by the complex value of the largest amplitude peak in the reference channel. This allows calibrated PRN radar echoes to be coherently integrated. Over long periods of time to increase the SNR, despite the instabilities of the transmitter. The antenna for this application has been investigated as well. It got a good return loss result and will be improved in the future.

6. ACKNOWLEDGEMENT

This research has been funded by ASPIRE 24N240 grant and United Arab Emirates University.

7. REFERENCES

[1] I. Barat *et al.*, "Radar Interference between C-band SAR Missions".

[2] F. J. Meyer, J. B. Nicoll, and A. P. Doulgeris, "Correction and characterization of radio frequency interference signatures in L-band synthetic aperture radar data," *IEEE Trans. Geosci. Remote Sens.*, vol. 51, no. 10, pp. 4961–4972, 2013, doi: 10.1109/TGRS.2013.2252469.

[3] S. W. Ellingson and J. T. Johnson, "A polarimetric survey of radio-frequency interference in C- and X-bands in the continental United States using WindSat radiometry," *IEEE Trans. Geosci. Remote Sens.*, vol. 44, no. 3, pp. 540–547, 2006, doi: 10.1109/TGRS.2005.856131.

[4] E. G. Njoku, P. Ashcroft, T. K. Chan, and L. Li, "Global survey and statistics of radio-frequency interference in AMSR-E land observations," *IEEE Trans. Geosci. Remote Sens.*, vol. 43, no. 5, pp. 938–946, 2005, doi: 10.1109/TGRS.2004.837507.

[5] "TerraSAR-X and TanDEM-X - Earth Online." Accessed: Mar. 06, 2024. [Online]. Available: https://earth.esa.int/eogateway/missions/terrasar-x-and-tandem-x

[6] "What is RADARSAT-2 | Canadian Space Agency." Accessed: Mar. 06, 2024. [Online]. Available: https://www.asc-csa.gc.ca/eng/satellites/radarsat2/what-is-radarsat2.asp

[7] "COSMO-SkyMed - Earth Online." Accessed: Mar. 06, 2024. [Online]. Available: https://earth.esa.int/eogateway/missions/cosmo-skymed

[8] "RISAT-1." Accessed: Mar. 06, 2024. [Online]. Available: https://www.isro.gov.in/RISAT_1.html

[9] "ALOS-2 / PALSAR-2." Accessed: Mar. 06, 2024. [Online]. Available: https://www.eorc.jaxa.jp/ALOS-2/en/about/palsar2.htm

[10] "Sentinel-1 - Missions - Sentinel Online - Sentinel Online." Accessed: Mar. 06, 2024. [Online]. Available: https://sentinels.copernicus.eu/web/sentinel/missions/sentinel-1

[11] "GF-3 (Gaofen-3) - eoPortal." Accessed: Mar. 06, 2024. [Online]. Available: https://www.eoportal.org/satellite-missions/gaofen-3#eop-quick-facts-section
[12] "SAOCOM (SAR Observation & Communications Satellite) - eoPortal." Accessed: Mar. 06, 2024. [Online]. Available: https://www.eoportal.org/satellite-missions/saocom
[13] "PAZ - Earth Online." Accessed: Mar. 06, 2024. [Online]. Available: https://earth.esa.int/eogateway/missions/paz
[14] "SAR data | ICEYE." Accessed: Mar. 06, 2024. [Online]. Available: https://www.iceye.com/sar-data
[15] "NovaSAR-1 - eoPortal." Accessed: Sep. 18, 2024. [Online]. Available: https://www.eoportal.org/satellite-missions/novasar-1#s-sar-s-band-synthetic-aperture-radar
[16] "SAR RCM | NOAA CoastWatch." Accessed: Mar. 06, 2024. [Online]. Available: https://coastwatch.noaa.gov/cwn/instruments/sar-rcm.html
[17] "What Is Software-Defined Radio (SDR)? - MATLAB & Simulink." Accessed: Mar. 07, 2024. [Online]. Available: https://www.mathworks.com/discovery/sdr.html
[18] A. Amézaga, C. López-Martínez, and R. Jové, "A multi-frequency sdr-based gbsar: System overview and first results," *Remote Sens.*, vol. 13, no. 9, pp. 1–19, 2021, doi: 10.3390/rs13091613.
[19] A. Vargas, R. Álvarez, P. Lupera, and F. Grijalva, "SDR-based Speed Measurement with Continuous-Wave Doppler Radar," *2021 IEEE Int. Mediterr. Conf. Commun. Networking, MeditCom 2021*, pp. 401–406, 2021, doi: 10.1109/MeditCom49071.2021.9647625.
[20] K. Hussein, A. S. I. Amar, A. Zekry, M. Abouelatta, A. K. Mahmoud, and M. Mabrouk, "Design and Implementation of SDR Platform for Radar Applications," *2023 Int. Telecommun. Conf. ITC-Egypt 2023*, pp. 372–375, 2023, doi: 10.1109/ITC-Egypt58155.2023.10206266.
[21] A. Prabaswara, A. Munir, and A. B. Suksmono, "GNU Radio based software-defined FMCW radar for weather surveillance application," *Proc. 2011 6th Int. Conf. Telecommun. Syst. Serv. Appl. TSSA 2011*, no. 144, pp. 227–230, 2011, doi: 10.1109/TSSA.2011.6095440.
[22] F. I. N. HARSWA, A. Rusdinar, R. M. Hidayat, and F. Y. Suratman, "Automatic Fish Feeder on Unmanned Surface Vehicle with Automatic Control and Navigation," *JMECS (Journal Meas. Electron. Commun. Syst.*, vol. 9, no. 1, pp. 1–9, Jun. 2022, doi: 10.25124/JMECS.V9I1.5285.
[23] "GNU Radio." Accessed: Sep. 18, 2024. [Online]. Available: https://wiki.gnuradio.org/index.php?title=Main_Page
[24] "bladeRF 2.0 micro - Nuand." Accessed: Mar. 18, 2024. [Online]. Available: https://www.nuand.com/bladerf-2-0-micro/